

## In vivo studies on toxin accumulation in liver and ultrastructural changes of hepatocytes of the phytoplanktivorous bighead carp i.p.-injected with extracted microcystins

Li Li, Ping Xie\*, Jun Chen

*Donghu Experimental Station of Lake Ecosystems, State Key Laboratory for Freshwater Ecology and Biotechnology of China, Institute of Hydrobiology, The Chinese Academy of Sciences, Donghu South Road 7, Wuhan 430072, People's Republic of China*

Received 29 January 2005; accepted 10 June 2005

Available online 8 August 2005

---

### Abstract

Phytoplanktivorous bighead carp were injected i.p. with extracted microcystins (mainly MC-RR and -LR) at two doses, 200 and 500 MC-LReq.  $\mu\text{g kg}^{-1}$  bw, and the changes in extractable MCs in liver and in the ultrastructure of hepatocytes were studied at 1, 3, 12, 24 and 48 h after injection. Quantitative and qualitative determinations of MCs in the liver were conducted by HPLC and LC-MS, respectively. MC concentration in the liver reached the maxima at 12 h ( $2.89 \mu\text{g MCs g}^{-1}$  dry weight at the lower dose) or at 3 h ( $5.43 \mu\text{g MCs g}^{-1}$  dry weight at the higher dose) post-injection, followed by sharp declines afterwards, whereas the ultrastructural changes of hepatocytes in both dose groups suggest progressive increases in severity toward the directions of apoptosis and necrosis from 1 to 24 h, respectively. There were two new findings in fish: widening of intercellular spaces was among the early ultrastructural changes induced by MCs and ultrastructural recovery of hepatocytes was evident at 48 h post-injection in both dose groups. Both the present and previous studies suggest that with in vivo or in vitro exposure to microcystins, hepatocyte damage in fish tends to proceed toward the direction of apoptosis at lower MC concentrations but toward the direction of necrosis at high MC concentrations. The temporal dynamics of MCs in the liver suggest that bighead carp may have a mechanism to degrade or bind MC-LR actively after it enters the blood system.

© 2005 Elsevier Ltd. All rights reserved.

*Keywords:* Microcystins; i.p.-injection; Hepatocyte; Bighead carp; Ultrastructural changes; Apoptosis; Necrosis

---

### 1. Introduction

Eutrophication of lakes and reservoirs leads to water blooms of cyanobacteria in many countries of the world. It is of great concern to human society because the bloom not only decreases water quality, but also increases the risk of toxicity to both animals and humans by producing microcystins (MCs) (Jochimsen et al., 1998; Falconer, 1999; Codd, 2000; Zimba et al., 2001). It is well known that

microcystins are potent inhibitors of protein phosphatases 1 and 2A (Eriksson et al., 1990; Falconer and Yeung, 1992; Runnegar et al., 1993) with liver as target organ. The high selectivity to liver is believed to be due to toxin uptake via bile acid carriers (Sahin et al., 1996). In instances of acute toxicity in mammals, liver damage and death result from hyperphosphorylation of cytoskeletal proteins secondary to protein phosphatase inhibition (Eriksson et al., 1990; Falconer and Yeung, 1992). This in turn results in hepatic necrosis, loss of hepatocyte cellular junction, and fatal intrahepatic hemorrhage (Hooser et al., 1990).

There have been only very limited in vivo studies on the toxic effects of microcystins on the ultrastructures of

---

\* Corresponding author. Tel./fax: +86 27 68780622.

E-mail address: xieping@ihb.ac.cn (P. Xie).

hepatocytes in fish, and the main ultrastructural changes induced by MCs in the omnivorous common carp and the carnivorous rainbow trout include swollen mitochondria, whirling of the rough ER, vacuolated cytoplasm, and condensed chromatin (Råbergh et al., 1991; Tencalla and Dietrich, 1997; Fischer et al., 2000; Li et al., 2004). However, no information was available for the phytoplanktivorous fishes that may be more frequently exposed to cyanobacterial toxins because of habitat and feeding mode. The studies on the dynamics of MCs in the tissues of silver carp fed with fresh toxic *Microcystis* suggest that phytoplanktivorous fish are probably more resistant to MC exposure than other fishes (Xie et al., 2004).

Bighead carp *Aristichthys nobilis* (Richardson), one of the most important freshwater phytoplanktivorous fish, comprises not only much of the production of Chinese aquaculture (Liang et al., 1981; Tang, 1981) but also a substantial proportion (e.g. 6% in 1989) of the total world catch in inland waters (FAO, 1991). Also, the filter-feeding fish are especially important to humans because of their roles in aquatic ecosystems as direct consumers of phytoplankton primary production, their importance as food fish and their potential for biological management of cyanobacterial blooms (Opuszynski and Shireman, 1995; Xie and Liu, 2001). Therefore, it is important to evaluate MC toxicity to this fish as well as the toxic impact on fish.

In the present study, bighead carp were injected i.p. with extracted microcystins (mainly MC-RR and -LR) at two doses, 200 and 500 MC-LReq.  $\mu\text{g kg}^{-1}$  bw. The purposes of this study were to describe the dynamics of extractable microcystin in liver over a period of 48 h, to evaluate the temporal changes in the ultrastructure of hepatocytes after injection with microcystins and to discuss the possible mechanisms underlying these patterns in comparison with mammals or other fishes of different feeding modes.

## 2. Materials and methods

### 2.1. Toxin

The freeze-dried cyanobacterial material used in the experiment was collected from Lake Dianchi, Yunnan of China. Before use, the material was analyzed for toxin content via reverse-phase high-performance liquid chromatography (HPLC) following the method of Fastner et al. (1998), and the microcystin content was  $1.41 \text{ mg g}^{-1}$  dry weight (DW), among which MC-RR, -LR and -YR were 0.84, 0.50 and  $0.07 \text{ mg g}^{-1}$  DW, respectively.

### 2.2. Fish

Bighead carp *Aristichthys nobilis* (Richardson) ( $n=36$ ) with mean weight  $51.27 \pm 1.76 \text{ g}$  were purchased from a local fish hatchery (Wuhan, China). Fish were acclimated

for 3 days prior to experimentation in 100-l aquaria containing dechlorinated tap water. Water temperature was  $20 \pm 1^\circ\text{C}$  and no food was given to the fish throughout the experiment.

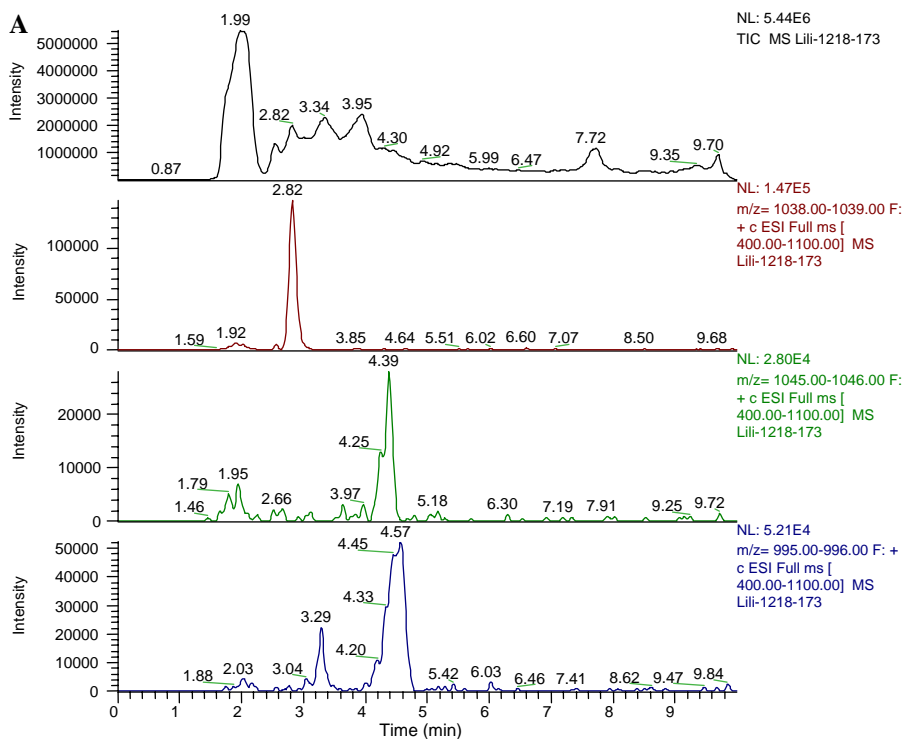
### 2.3. Sample preparation

Crude algae were freeze-dried and then extracted with methanol, and finally suspended in distilled water. The doses of approximately 0.5 ml suspension of extracted solution of microcystins in plain distilled water were directly injected (i.p.) along the ventral midline into the peritoneum using syringes, amounting to equivalent of 400 and 1000  $\mu\text{g MC-LR} + \text{MC-RR}$  per kg body weight (bw). Gupta et al. (2003) reported 24 h  $\text{LD}_{50}$  (i.p.) doses of MC-LR, RR and YR in mice are 43, 235.4 and  $110.6 \mu\text{g kg}^{-1}$  body weight, respectively. Thus the toxicity of MC-RR and MC-YR in mice is nearly one fifth and one third of MC-LR, respectively. Comparably, the doses of 400 and 1000  $\mu\text{g kg}^{-1}$  injected with extracted compound toxins of MC-LR and MC-RR in this study, according the toxicity of MC-LR and MC-RR, are equivalent to 200 and 500  $\mu\text{g kg}^{-1}$  purified MC-LR, respectively.

Three test fish in both dose groups were killed at 1, 3, 12, 24 and 48 h post-injection, respectively. Three control fish killed only at 0 and 48 h. Liver samples were excised, freed of attached tissue, and then weighed.

### 2.4. Determination of MC concentration in liver

Extraction and analysis of the microcystins in the fish liver followed the method of Xie et al. (2004). Briefly, lyophilized samples were weighed, and then homogenized and extracted three times with 10 ml of BuOH: MeOH:  $\text{H}_2\text{O}$  (1:4:15) for 24 h while stirring. The extract was centrifuged and the supernatant was diluted with water. This diluted extract was directly applied to a  $\text{C}_{18}$  reversed phase cartridge, which had been preconditioned by washing with methanol and distilled water. The column was washed with water and 25% methanol. Elution from the column with 90% methanol yielded the toxin-containing fraction. The toxin-containing fraction was evaporated to dryness. Then the residue was dissolved with methanol and then eluted with 70% methanol, the toxin-containing fraction was also evaporated to dryness. This fraction was dissolved with methanol and the methanol solution was subjected to HPLC. A gradient starting at 50% (v/v) aqueous methanol with 0.05% trifluoroacetyl (TFA) was increased to 70% (v/v) in 25 min at a flow rate of 1 ml/min. MC concentrations in fish livers were determined by comparing the peak areas of the test samples with those of the standards available (MC-LR, MC-RR and MC-YR, Wako Pure Chemical Industries, Japan). Qualitative analysis of MCs was performed using a Finnigan LC-MS system. The LC-MS conditions were as follows: ESI spray voltage 4.54 kV, sheath gas flow rate



Lili-1218-173 #211 RT: 2.81 AV: 1 NL: 2.32E5  
T: + c ESI Full ms [ 400.00-1100.00]

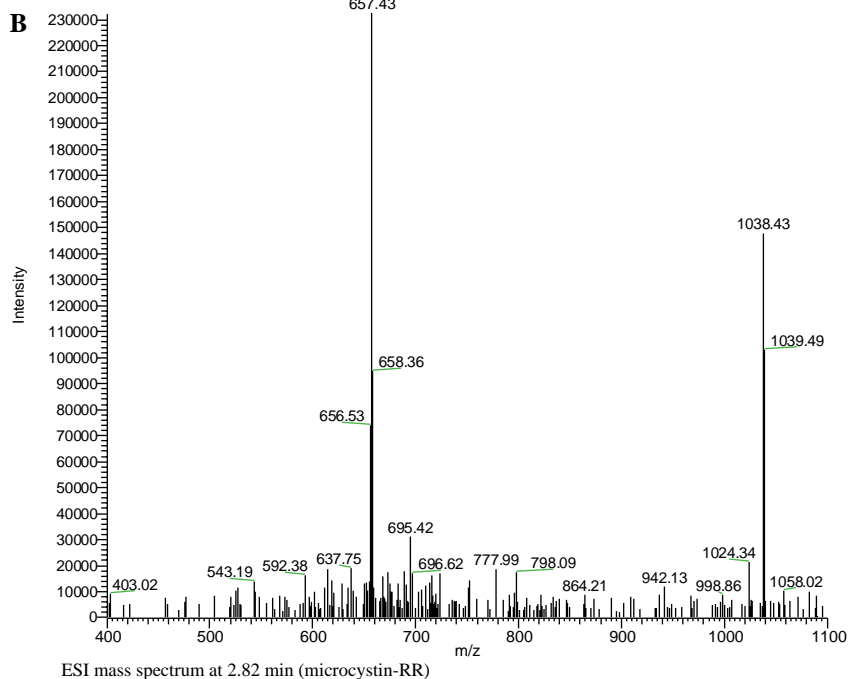


Fig. 1. ESI LC/MS analysis of microcystins in liver of bighead carp in the 500  $\mu\text{g kg}^{-1}$  dose group at 3 h post-injection. Mass chromatograms monitored at  $m/z$  1038, 995, 1045 (A), ESI mass spectrum at 2.82 min (microcystin-RR) (B), ESI mass spectrum at 4.57 min (microcystin-LR) (C) and 4.39 min (microcystin-YR) (D).

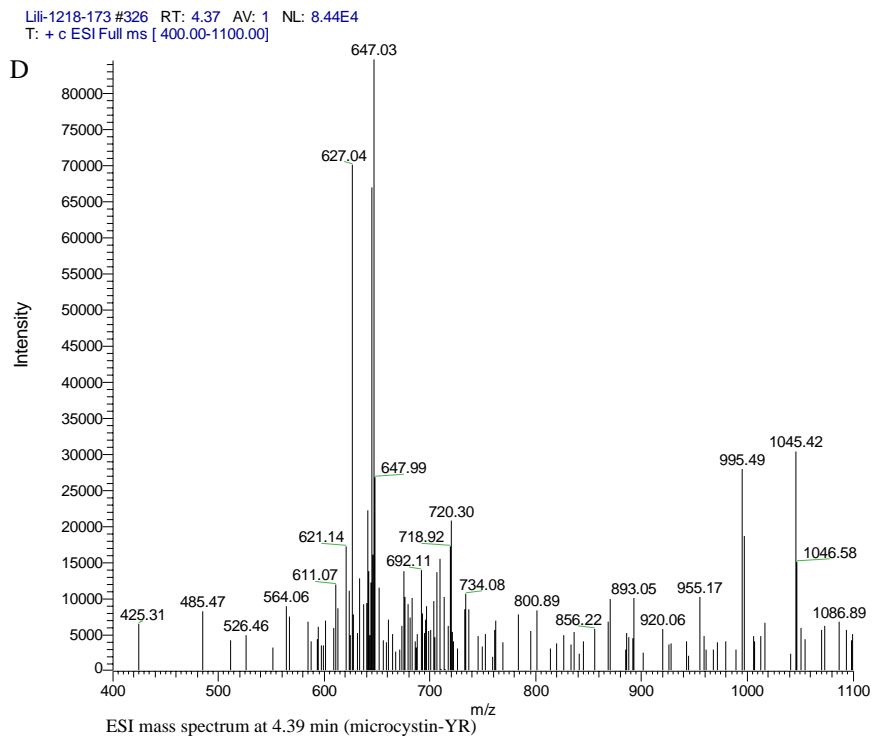
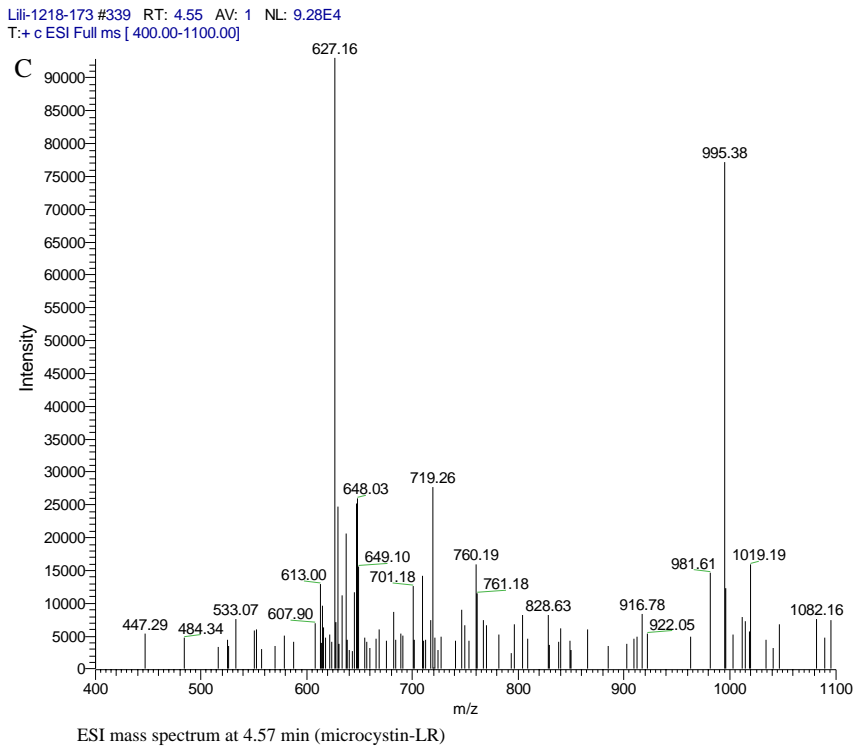


Fig. 1 (continued)

30 unit, auxiliary gas flow rate 0 unit, capillary voltage 45.67 V, capillary temperature 230 °C, and multiplier voltage –801.62 V.

### 2.5. Transmission electron microscopic observation

For transmission electron microscopic study, specimens of the liver tissues were prefixed in 2.5% glutaraldehyde solution, diced into 1 mm<sup>3</sup>, followed by three 15 min rinses with 0.1 M phosphate buffer (pH 7.4). Post-fixation was in cold 1% aqueous osmium tetroxide for 1 h. After rinsing with phosphate buffer again, the specimens were dehydrated in a graded ethanol series of 50–100% and then embedded in Epon 812. Ultra-thin sections were sliced with glass knives on a LKB-V ultramicrotome (Nova, Sweden), stained with uranyl acetate and lead citrate and examined under a HITACHI, H-600 electron microscope.

## 3. Results

### 3.1. Dynamics of MCs in liver

Fig. 1 shows the ESI LC/MS analysis of microcystins in liver of bighead carp in the 500 µg kg<sup>-1</sup> dose group at 3 h post-injection. Based on total ion chromatogram, mass chromatograms monitored at *m/z* 1038, and the presence of [M+H]<sup>+</sup> ion at *m/z* 1038, it is confirmed that the peak at 2.82 min was derived from MC-RR. Similarly, the peak at 4.57 min was deduced to be derived from MC-LR, as the peak was detected by monitoring with *m/z* 995, and the mass chromatogram showed [M+H]<sup>+</sup> ion at *m/z* 995. Since MC-YR in bighead carp livers was so rare that the mass chromatograms monitored at *m/z* 1045 was obscure.

In the 200 µg MC-LReq. kg<sup>-1</sup> dose group, MC concentration in liver varied between 0 and 2.89 µg g<sup>-1</sup> DW. Due to an accidental mistake in the extraction procedure, we failed to detect any microcystin at 3 h post-injection in the 200 µg kg<sup>-1</sup> dose group (Fig. 2(a)). In the 500 µg MC-LReq. kg<sup>-1</sup> dose group, MCs varied between 0.25 and 5.43 µg g<sup>-1</sup> DW, and after reaching a maximum at 3 h post-injection, it decreased from 12 to 48 h post-injection (Fig. 2(b)).

### 3.2. Ultrastructural changes

#### 3.2.1. Intercellular junction

Sections derived from the control fish had intact plasmalemma and distinct cell junctions (Fig. 3(A)). After 1 h, widening of intercellular spaces was firstly noticed in both dose groups (Fig. 3(B) and (C)). At 3 h, the gaps became wider in the 200 µg kg<sup>-1</sup> dose group (Fig. 3(D)). Disassociation of hepatocytes and loss of desmosomes were observed in the 500 µg kg<sup>-1</sup> dose group at 3 h post-injection. Furthermore, many erythrocytes were observed in

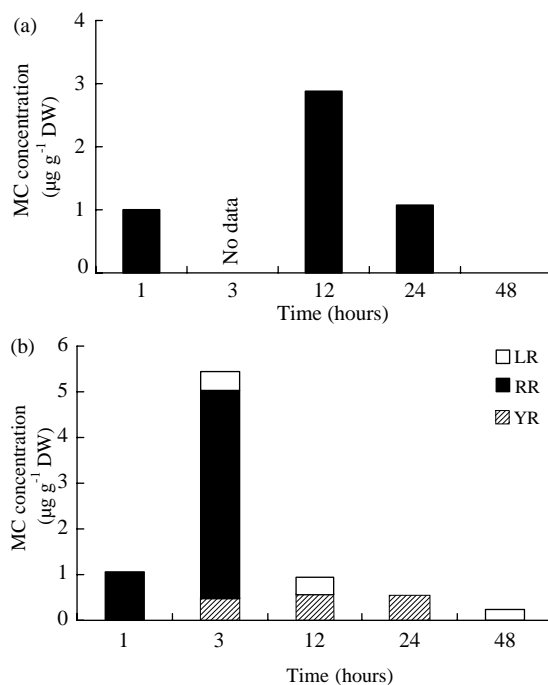


Fig. 2. MC concentration in liver of bighead carp after i.p. injection with microcystins equivalent to (a) 200 and (b) 500 µg MC-LReq. kg<sup>-1</sup> bw, respectively.

the dilated non-cellular space in the 500 µg kg<sup>-1</sup> dose group (Fig. 3(E)). After 12 h, we observed, in both dose groups, losses of normal intercellular junctions and marked disassociation of hepatocytes with disrupted hepatic cords, which was accompanied consequently with intrahepatic hemorrhage (Fig. 4(A)). At 48 h post-injection, the hepatocytes recovered in both dose groups (Fig. 3(F)), whereas the recovery was more apparent in the 200 µg kg<sup>-1</sup> than in the 500 µg kg<sup>-1</sup> dose groups (Fig. 3(G)).

#### 3.2.2. Cell membrane

Most hepatocytes maintained their normal morphology in the 200 µg kg<sup>-1</sup> dose group at 1 h post-injection. At 3 h, membranes of some hepatocytes began to bleb and such blebbing became more serious with the disassociation of hepatocytes in the 200 µg kg<sup>-1</sup> dose group (Fig. 4(A)). At 24 h, membrane blebbing in most hepatocytes were more prominent, and many membrane-bound plasma membrane blebs were observed to pinch off from the cell surface, containing redistributed and compacted cytoplasmic organelles. Furthermore, some cells disintegrated into small membrane-bound fragments (Fig. 4(B)). In contrast, in the 500 µg kg<sup>-1</sup> dose group, the cells became round and swollen with time, and disruption and lysis of cell membrane were observed in most hepatocytes at 24 h (Fig. 4(C) and (D)). However, cell membranes showed great recovery at 48 h in both dose groups (Fig. 3(F) and (G)).

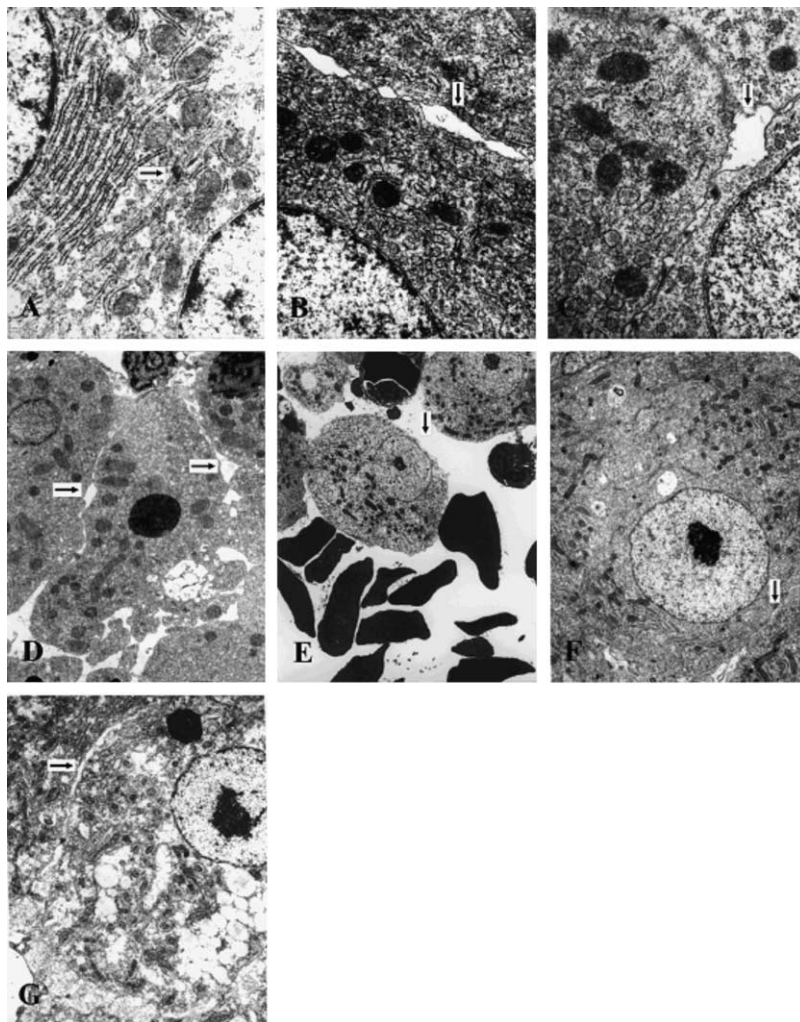


Fig. 3. Toxic effects of MCs on intercellular junctions of hepatocytes from bighead carp after injection with 200 and 500  $\mu\text{g MC-LR kg}^{-1}$  bw, respectively. (A) cellular junctions (desmosomes) of control fish, 17,000 $\times$ . (B) and (C) showing the dilation of intercellular space in the 200 and 500  $\mu\text{g MC-LR kg}^{-1}$  dose groups at 1 h post-injection, respectively, 17,000 $\times$ . (D) and (E) showing the widening of intercellular space in the 200 and 500  $\mu\text{g MC-LR kg}^{-1}$  dose groups at 3 h post-injection, respectively, 6000 $\times$ . (F) and (G) showing the recovery hepatocyte in the 200 and 500  $\mu\text{g MC-LR kg}^{-1}$  dose groups at 48 h post-injection, respectively, intercellular space (arrow), 6000 $\times$ .

### 3.2.3. Smooth and rough endoplasmic reticulum

In the control fish, the hepatocytes had stacks of RER concentrating around the cell nuclei and the cell membrane borders (Fig. 5(A)). In the 200  $\mu\text{g kg}^{-1}$  dose group, modification of RER and SER was not significant since whirling of RER at the periphery of plasma membrane were present at 24 h (Fig. 5(B)), while at 48 h, normal smooth and rough ER were commonly observed (Fig. 3(F)). However, there was a widespread swelling of RER and SER in the 500  $\mu\text{g MC-LR kg}^{-1}$  dose group within 24 h post-injection. At 24 h, dilation and vesiculation of cisternae of endoplasmic reticulum were most prominent (Fig. 5(C)), partial or total loss of ribosomes of RER was observed, and furthermore, some dilated part of RER was transformed

into vesicles by fragmentation or separation. At 48 h, both dispersed RER and SER showed substantial recovery in the 500  $\mu\text{g kg}^{-1}$  dose group.

### 3.2.4. Mitochondria

In the 200  $\mu\text{g kg}^{-1}$  dose group, mitochondria did not change evidently within 24 h post-injection, and only at 24 h, the densely stained mitochondria presented dilated cristae (Fig. 6(A) and (B)). However, in the 500  $\mu\text{g kg}^{-1}$  dose group, the mitochondria proceeded to lose cristae and matrix in a progressive, time-dependent manner (Fig. 6(C) and (D)), and lost their metrical density with highly hydropic changes at 24 h (Fig. 6(D)). At 48 h, most mitochondria showed considerable recovery with only

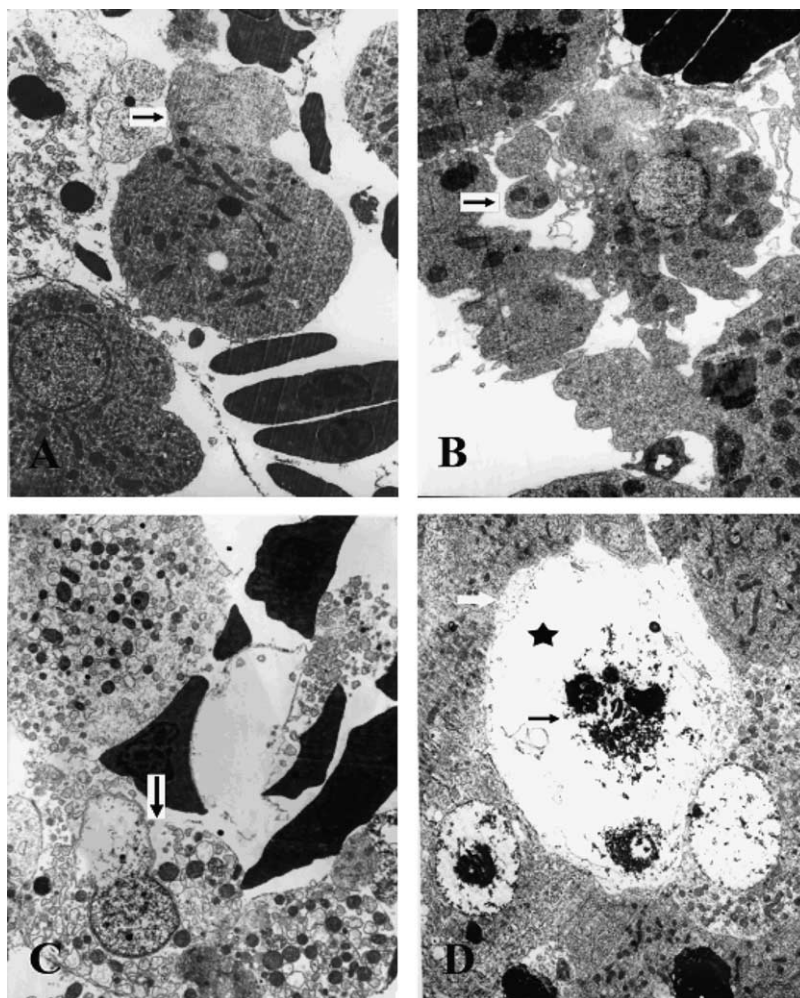


Fig. 4. Toxic effects of MCs on the cell membrane of hepatocytes from bighead carp after injection with 200 and 500  $\mu\text{g MC-LR kg}^{-1}$  bw, respectively. (A) and (B) showing the blebbing of cell membrane and pinched off bodies (arrow) in the 200  $\mu\text{g MC-LR kg}^{-1}$  dose group at 12 and 24 h post-injection, respectively, 4000 $\times$ , 6000 $\times$ . (C) showing disrupted cellular membrane (arrow) at 500  $\mu\text{g MC-LR kg}^{-1}$  dose group at 24 h post-injection, 3000 $\times$ . (D) showing dissolving cellular membrane (white arrow), fragmentation of nuclear (black arrow) and loss of cytoplasm (asterisk) in the 500  $\mu\text{g MC-LR kg}^{-1}$  dose group at 24 h post-injection, 4000 $\times$ .

slightly swollen forms present in both dose groups (Fig. 3(F) and (G)).

### 3.2.5. Nuclear

Morphologic alterations in nuclei became most prominent in both dose groups within 24 h post-injection. In the 200  $\mu\text{g MC-LR kg}^{-1}$  dose group, the toxins induced a progressive deformation of the nuclear outline (Fig. 7(B)), and at 24 h, there was a prominent decrease in the amount of homochromatin with compaction of heterochromatin, eventually resulting in a highly electronlucent nucleoplasm (Fig. 7(C)). However, in the 500  $\mu\text{g MC-LR kg}^{-1}$  dose group nuclei were highly condensed and fragmented (Fig. 4(D)), and the nucleolus could no longer be discerned in some hepatocytes (Fig. 7(D)). Also, the large and round

nuclei were seen in the center of hepatocytes in both dose groups at 48 h post-injection (Fig. 3(F) and (G)).

### 3.2.6. Cytoplasm

In the hepatocytes of the control fish, we observed normal ultrastructures of the endoplasmic reticulum, mitochondria and other organelles (Fig. 8(A)). In the 200  $\mu\text{g kg}^{-1}$  dose group, the cell shrunk and cytoplasm became deep as the time went on. The organelles were redistributed at 24 h post-injection (Fig. 4(B)). In the 500  $\mu\text{g MC-LR kg}^{-1}$  dose group, the cell became rounding with light cytoplasm within 24 h post-injection. Some vacuoles were frequently seen in cytoplasm at 24 and 48 h post-injection (Figs. 8(B) and 3(G)), even with complete loss of cytoplasm (Fig. 4(D)). Furthermore, the vacuoles often

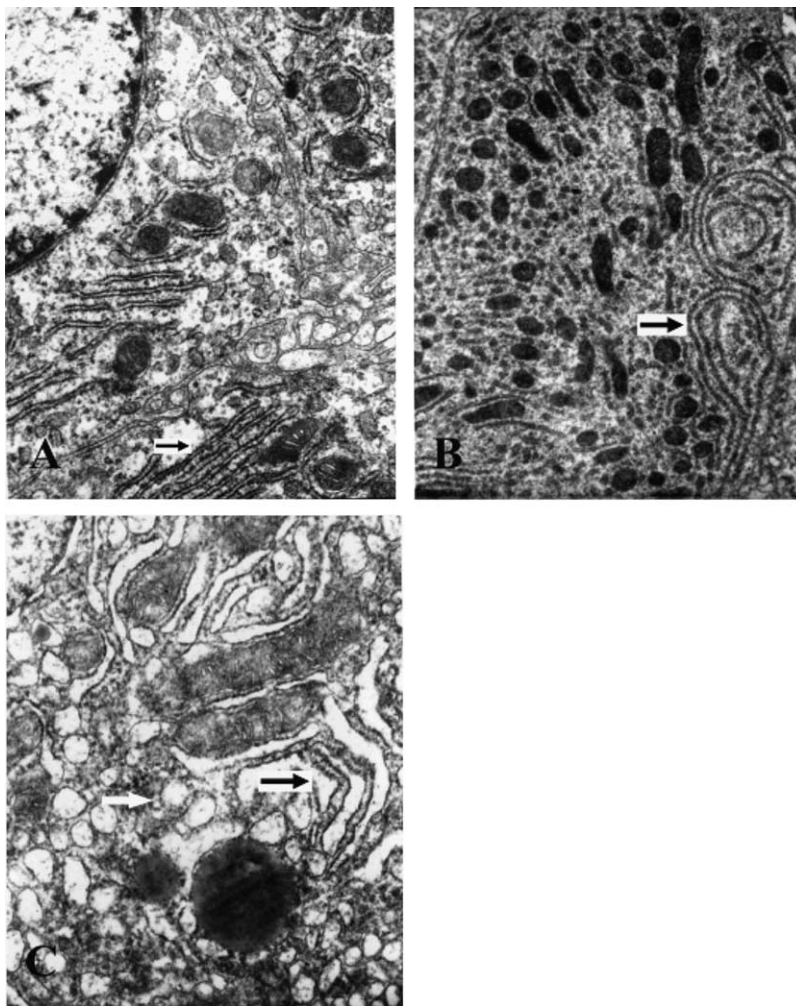


Fig. 5. Toxic effects of MCs on the ER of hepatocytes from bighead carp after injection with 200 and 500  $\mu\text{g MC-LR kg}^{-1}$  bw, respectively. (A) RER of control fish, 17,000 $\times$ . (B) showing the whirling of RER in the 200  $\mu\text{g MC-LR kg}^{-1}$  dose group at 24 h post-injection, 8000 $\times$ . (C) showing the vesiculation of SER (white arrow) and the swelling and degranulation of RER (black arrow) in the 500  $\mu\text{g MC-LR kg}^{-1}$  dose group at 24 h post-injection, 17,000 $\times$ .

contained concentric layers of membranes, resembling myelinated bodies (Fig. 8(C)). At 48 h, the cytoplasm became dense in the 200  $\mu\text{g kg}^{-1}$  dose group, and there were numerous various-sized lipid droplets with massive lipofusins present in the 500  $\mu\text{g MC-LR kg}^{-1}$  dose group (Fig. 8(D)).

#### 4. Discussion

In the present study, bighead carp injected with extracted microcystins demonstrated time-dose dependent ultrastructural changes in the liver within 24 h post-injection: widening of intercellular spaces was firstly noticed at 1 h in both dose groups and the gaps became more widening at 3 h; between 3 and 12 h, the hepatocytes showed cellular

membranes blebbing, cytoplasm condensation and chromatin compaction in the 200  $\mu\text{g kg}^{-1}$  dose group, but became large and round with swollen organelles in the 500  $\mu\text{g kg}^{-1}$  dose group; at 24 h, membrane blebbing and nuclear deformation were most prominent with appearance of some 'apoptotic bodies' in the 200  $\mu\text{g kg}^{-1}$  dose group, but disruption and lysis of cell membrane and fragmentation of nuclear were predominant in the 500  $\mu\text{g kg}^{-1}$  dose group; and at 48 h, most hepatocytes showed ultrastructural recovery in both dose groups. It is well known that blebbing of cell membrane and appearance of apoptotic bodies are typical ultrastructural features of apoptosis (Kerr et al., 1972; Wyllie et al., 1980; Khan et al., 1995; McDermott et al., 1998; Li et al., 2001). In our study, the typical ultrastructural changes (such as cell membrane blebbing, deformation of the nucleus, compaction of chromatin, and



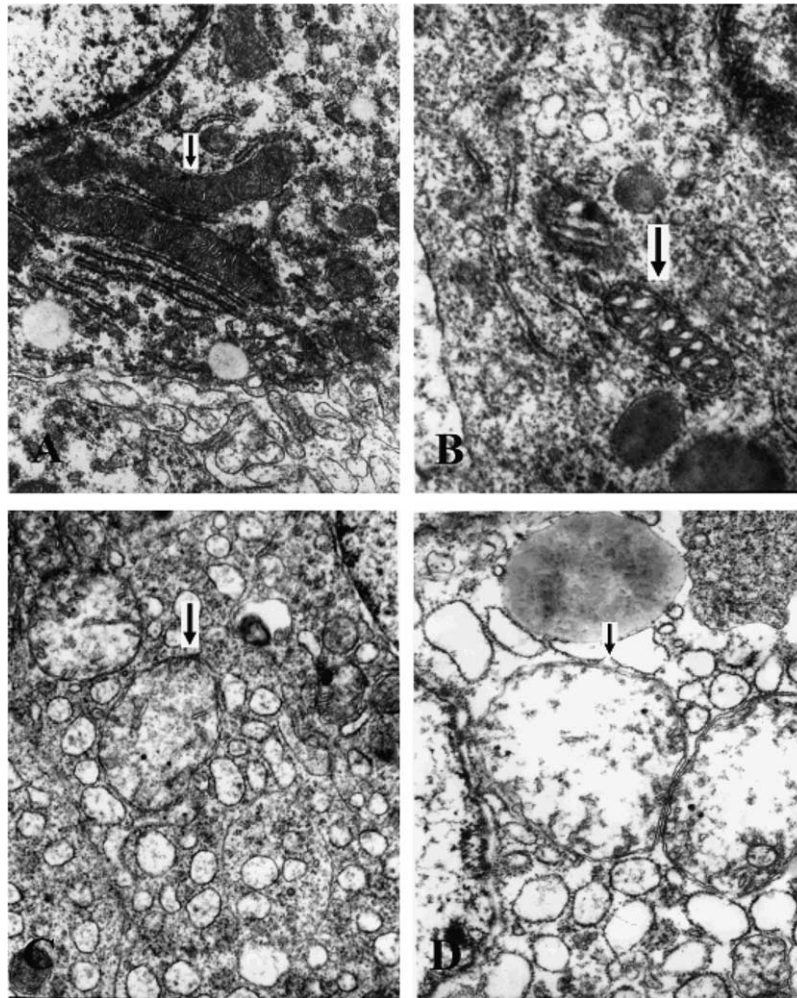


Fig. 6. Toxic effects of MC on the mitochondria of hepatocytes from bighead carp after injection with 200 and 500  $\mu\text{g MC-LR kg}^{-1}$  bw, respectively. (A) mitochondria of control fish, 17,000 $\times$ . (B) showing dilation of mitochondrial cristae in the 200  $\mu\text{g MC-LR kg}^{-1}$  dose group at 24 post-injection, 8000 $\times$ . (C) and (D) showing the swelling and vesiculation of mitochondria in the 500  $\mu\text{g MC-LR kg}^{-1}$  dose group at 12 h and 24 post-injection, respectively, both in 17,000 $\times$ .

pinching off membrane blebs-apoptotic bodies) of hepatocytes in the 200  $\mu\text{g MC-LR kg}^{-1}$  dose group were evidently compatible with characters of cell apoptosis; whereas the ultrastructural changes (such as cell swelling, organelles distended or even disrupted, followed by a cell death) of hepatocytes in the 500  $\mu\text{g MC-LR kg}^{-1}$  dose group were consistent with the symptoms of cell necrosis (Slauson and Cooper, 1982). In vivo cell apoptosis or necrosis has been previously observed in mammals (Dabholkar et al., 1987; Miura et al., 1989; Ito et al., 1997) and in fish (Kotak et al., 1996; Tencalla and Dietrich, 1997; Fischer et al., 2000; Li et al., 2004). In vitro, isolated rat hepatocytes displayed apoptosis when exposed to low MC-LR concentrations (0.8–2  $\mu\text{M}$ ) but necrosis when exposed to high MC-LR concentrations (25–50  $\mu\text{M}$ ) (McDermott et al., 1998). Li et al. (2001) administered MC-LR to isolated hepatocytes

of common carp and observed ultrastructural changes of apoptosis and necrosis when the cells were exposed to 50 and 500 MC-LR  $\mu\text{g/L}$  for 8 h, respectively. Therefore, our results together with previous studies suggest that whenever in vivo or in vitro exposure to microcystins, hepatocyte damage in fish or mammals tends to proceed toward the direction of apoptosis at lower MC concentrations but toward the direction of necrosis at high MC concentrations.

There were only a few in vivo studies to document ultrastructural changes of fish hepatocytes after exposure to MCs. A subchronic dose (50  $\mu\text{g MC-LR kg}^{-1}$ ) was orally administered to common carp by feeding with bloom scum, and after 28 days, ultrastructural changes of livers were observed: swollen endomembrane system, dilation of cisternae of the rough ER and ER transformation into concentric membrane whorls, and numerous electron-lucent

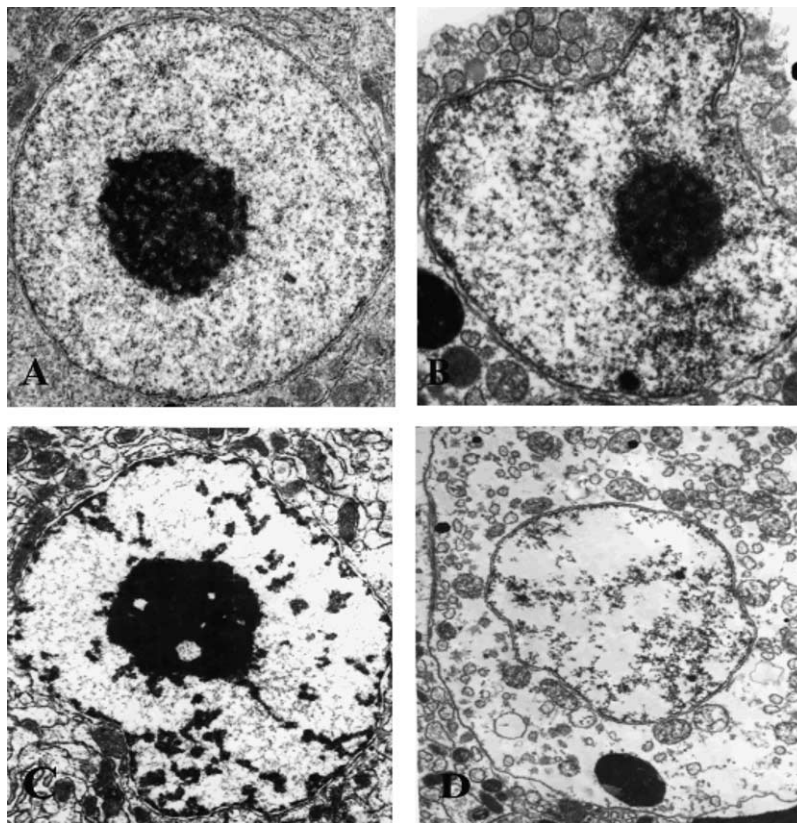


Fig. 7. Toxic effects of MC on the nuclei of hepatocytes from bighead carp after injection with 200 and 500  $\mu\text{g MC-LR kg}^{-1} \text{ bw}$ , respectively. (A) nucleus of control fish 10,000 $\times$ . (B) and (C) showing the deformation of nuclei and condensation of chromatin in the 200  $\mu\text{g MC-LR kg}^{-1}$  dose group at 24 h post-injection, 10,000 $\times$  and 6000 $\times$ . (D) showing the necrosis of cell in the 500  $\mu\text{g MC-LR kg}^{-1}$  dose group at 24 h post-injection, 6000 $\times$ .

membrane-bound vacuoles (Li et al., 2004). Common carp were injected i.p. with a sublethal dose of MC-LR (150  $\mu\text{g MC-LR kg}^{-1}$ ), which resulted in disassociation of hepatocytes, vacuolization of cytoplasm at 0.5 h post-injection, dispersion of the stacks of rough ER and mitochondria throughout the cytoplasm and the presence of a concentration of microfilaments at the intercellular space at 1 h post-injection, with highly vesiculated rough ER at 6 h post-injection (Råbergh et al., 1991). Rainbow trout were gavaged with freeze-dried toxic cells of *Microcystis aeruginosa* at a dose of 5700  $\mu\text{g MC-LR kg}^{-1} \text{ bw}$ , which caused ultrastructural changes of massive necrosis of the liver: at 1 h after gavage, there were changes in small, well-defined areas where the typical chord structure of trout liver disappeared with appearance of condensed cytoplasm, between 3 and 12 h, nuclei began to condense with highly vacuolated cytoplasm, and after 24–48 h, membranes were lysed and nuclei were pyknotic, and such ultrastructural damage extended to the whole liver (Tencalla and Dietrich, 1997). Some of these alterations are consistent with our observation, but we found widening of intercellular spaces among the early ultrastructural changes induced by MCs,

which is the first report in fish. In mammals, the widening of intercellular spaces is presumed to be a critically important effect of the toxin and is related to the disruption by MC-LR of microtubules (MTs), cytokeatin intermediate filaments (IFs) and microfilaments (MFs) (Wickstrom et al., 1995, 1996; Khan et al., 1996). It is likely that the widening of intercellular spaces observed in bighead livers in this present study might have resulted from toxin-induced destabilization of adhesive structures through increased phosphorylation (Eriksson et al., 1990; Falconer and Yeung, 1992). It is known that microcystins are potent and specific inhibitors of PP1 and PP2A, which disturbs the cellular phosphorylation balance and causes hyperphosphorylation of a variety of proteins (Eriksson et al., 1990; Falconer and Yeung, 1992; Runnegar et al., 1993). These proteins (e.g. actin, talin or  $\alpha$ -actin) are certainly responsible for alterations in the loss of normal cell shape, the widening of intercellular spaces and disassociation of hepatocytes, which finally leads to apoptosis and/or necrosis of hepatocytes (Dawson, 1998). Similarly, when cultured rat hepatocytes were exposed to microcystins, the first action point of MC was also the intercellular junctions

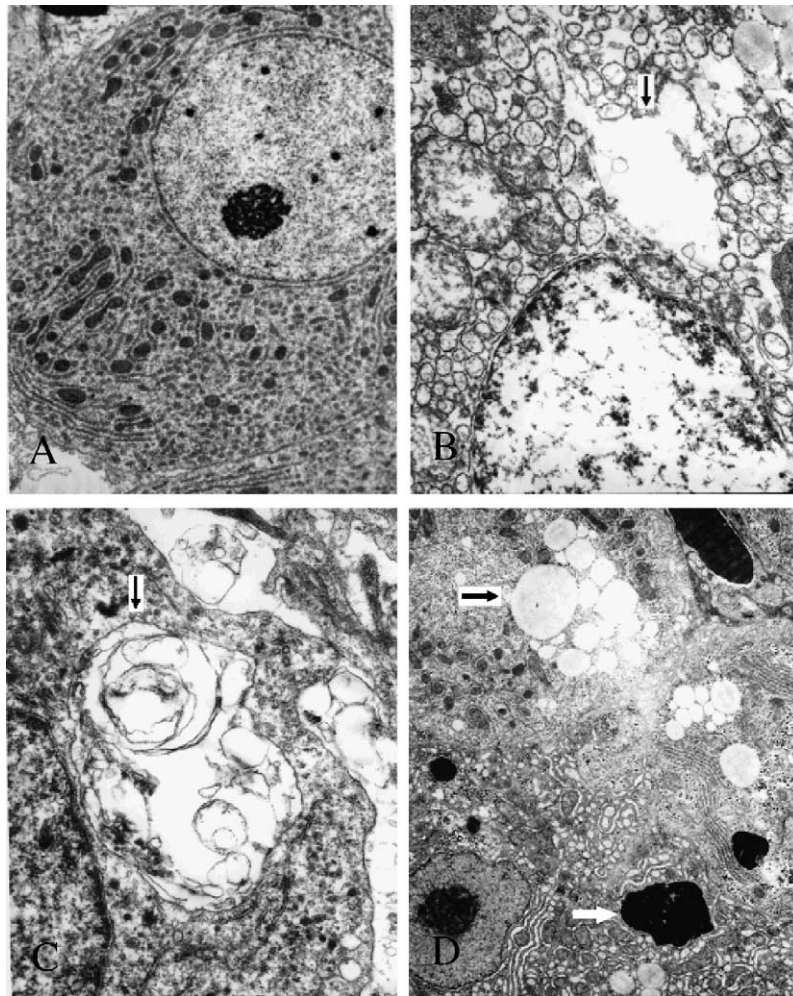


Fig. 8. Toxic effects of MC on cytoplasm of hepatocytes from bighead carp after injection with 200 and 500  $\mu\text{g MC-LR kg}^{-1}$  bw, respectively. (A) the control cell, 6000 $\times$ . (B) showing the vacuoles in the 500  $\mu\text{g MC-LR kg}^{-1}$  dose group at 24 h post-injection, 10,000 $\times$ . (C) showing the formation of myeloid-like bodies in the 500  $\mu\text{g MC-LR kg}^{-1}$  dose group at 48 h post-injection, 17,000 $\times$ . (D) showing the presence of lipid droplets (black arrow) and lipofuscins (white arrow) in the 500  $\mu\text{g MC-LR kg}^{-1}$  at 48 h post-injection, 4000 $\times$ .

(Wickstrom et al., 1996). Therefore, evidence from both fish and mammals indicates that MCs act firstly on the intercellular junctions of hepatocytes in animal livers.

In the present study, with a remarkable decrease or even disappearance of MCs in the liver at 48 h post-injection, ultrastructural recovery of hepatocytes was evident in both dose groups. This is the first report on ultrastructural recovery of fish liver exposed to MCs. Malbrouck et al. (2003) observed recovery of liver under light microscopy in goldfish *Carassius auratus*, injected with a dose of 125  $\mu\text{g MC-LR kg}^{-1}$  bw: recovery of the tissue structure and regeneration of hepatocytes were visible after 96 h, and there was a reconstruction of initial tissue structure (only few inflammatory regions persisted) after 21 days post-injection. Compared with goldfish, bighead carp showed more quick recovery in spite of exposure to higher MC

doses. Such differences in response to MC exposure are most likely due to different detoxification among different fish species, since phytoplanktivorous fishes like silver and bighead carps are possibly more tolerant to high microcystins than other fishes from an evolutionary point of view (Xie et al., 2004).

In the present study, MC concentration in the liver of bighead carp reached the maxima at 3 or 12 h post-injection, followed by a sharp decline afterwards, whereas the ultrastructural changes of hepatocytes in both dose groups progressively increased in severity toward the directions of apoptosis and necrosis from 1 to 24 h, respectively. Similarly, in rainbow trout gavaged with freeze-dried toxic cells of *Microcystis aeruginosa* at 5700  $\mu\text{g MC-LR kg}^{-1}$  bw, MC concentration in liver reached the maximum (524 ng/g liver) at 3 h post-injection,

then showed quick declines within 24 h and remained low during 24–48 h, whereas liver ultrastructural damage continued to progress with time (Tencalla and Dietrich, 1997). Apparently, there is a delay in the ultrastructural changes related to peak accumulation of microcystins in fish liver. Fischer et al. (2000) indicate that the decrease of extractable MC concentration after peak accumulation in liver may be attributed to two factors: one is biliary excretion of MC or its metabolites (Sahin et al., 1996), the other is the slow covalent addition of MC to the catalytic subunit of PP and other thiol containing cellular proteins (Hitzfeld et al., 1999), which may contribute to the progressive necrosis of hepatocytes.

In the present study, although it comprised 35.5% of the total toxins i.p.-injected to bighead carp, MC-LR in the liver was not detected at the 200 µg MC-LR kg<sup>-1</sup> dose group, but was rather low at the 500 µg MC-LR kg<sup>-1</sup> dose group within 24 h. In a subchronic toxicity experiment where the phytoplanktivorous silver carp were fed with toxic fresh *Microcystis viridis* cells (MC-RR and -LR contents were 268–580 and 110–292 µg g<sup>-1</sup> DW, respectively), MC-LR were almost not detectable in the fish liver, and it is suggested that silver carp may have a mechanism to degrade MC-LR actively in the intestines and to inhibit MC-LR transportation across the intestines (Xie et al., 2004). The present results suggest that bighead carp may have a mechanism to degrade or bind MC-LR actively after it enters the blood system. Detailed studies are needed in our future research to clarify the degradation mechanisms of the most toxic MC-LR in the phytoplanktivorous fishes.

### Acknowledgements

The authors would like to thank Dr Zheng L of the Donghu Experimental Station of Lake Ecosystems, Institute of Hydrobiology, for his assistance in the experiment. Thanks are also due to Dr Alan Harvey and two anonymous reviewers for useful comments and suggestions. This work was supported by the Key Project of CAS titled 'The effects of the regenerative organic pollutant microcystins on the safety of aquatic food' (KSCX2-SW-129) and by a fund from the National Natural Science Foundation of China (30225011).

### References

Codd, G.A., 2000. Cyanobacterial toxins, the perception of water quality, and the prioritization of eutrophication control. *Ecol. Eng.* 16, 51–60.

Dabholkar, A.S., Carmichael, W.W., 1987. Ultrastructural changes in the mouse liver induced by hepatotoxin from the freshwater cyanobacterium *microcystis aeruginosa* strain 7820. *Toxicol* 25, 285–292.

Dawson, R.M., 1998. The toxicology of microcystins. *Toxicol* 36, 953–962.

Eriksson, J.E., Toivola, D., Meriluoto, J.A.O., Karaki, H., Han, Y., Hartshorne, D., 1990. Hepatocyte deformation induced by cyanobacterial toxin reflects inhibition of protein phosphatases. *Biochem. Biophys. Res. Commun.* 173, 1347–1353.

Falconer, I.R., 1999. An overview of problem caused by toxic blue-green algae (*Cyanobacteria*) in drinking and recreational water. *Environ. Toxicol.* 14, 5–12.

Falconer, I.R., Yeung, D.S.K., 1992. Cytoskeletal changes in hepatocytes induced by Microcystis toxins and their relation to hyperphosphorylation of cell proteins. *Chem. Biol. Interact.* 81, 181–196.

FAO, 1991. Anon., 1991. Fishery Statistics, Catches and Landing, FAO Yearbook. Food and Agriculture Organization of the United Nations, Rome.

Fastner, J., Flieger, I., Neumann, U., 1998. Optimised extraction of microcystins from field sample-A comparison of different solvents and procedures. *Water Res.* 32, 3177–3181.

Fischer, W.J., Hitzfeld, B.C., Tencalla, F., Eriksson, J.E., Mikhailov, A., Dietrich, D.R., 2000. Microcystin-LR toxicodynamics, induced pathology, and immunohistochemical location in livers of blue-green algae exposed rainbow trout (*Oncorhynchus mykiss*). *Toxicol. Sci.* 54, 365–372.

Gupta, N., Pant, S.C., Vijayaraghavan, R., Lakshmana Rao, P.V., 2003. Comparative toxicity evaluation of cyanobacterial cyclic peptide toxin microcystin variants (LR, RR, YR) in mice. *Toxicology* 188, 285–296.

Hitzfeld, B., Fischer, W., Eriksson, J., Mikhailov, A., Tencalla, F., Dietrich, D.R., 1999. Toxins of cyanobacteria in fish: immunohistochemical and immunocytochemical localization in livers and hepatocytes of rainbow trout. *Naunyn-Schmiedeberg's Arch. Pharmacol.* 359, R159.

Hooser, S.B., Beasley, V.R., Basgall, E.J., Carmichael, W.W., Haschek, W.M., 1990. Microcystin-LR-induced ultrastructural changes in rats. *Vet. Pathol.* 27, 9–15.

Ito, E., Kondo, F., Harada, K-I., 1997. Hepatic necrosis in aged mice by oral administration of microcystin-LR. *Toxicol* 35, 231–239.

Jochimsen, E.M., Carmichael, W.W., An, J., Cardo, D.M., Cookson, S.T., Holmes, C.E.M., Antunes, M.B.C., Filho, D.A.M., Lyra, T.M., Barreto, V.S.T., Azevedo, S.M.F.O., Jarvis, W.R., 1998. Liver failure and death after exposure to microcystins at a hemodialysis center in Brazil. *New. Engl. J. Med.* 338, 873–878.

Khan, S.A., Ghosh, S., Wickstrom, M., Miller, L.A., Hess, R., Haschek, W., Beasley, V.R., 1995. Comparative pathology of microcystin-LR in cultured hepatocytes, fibroblasts, and renal epithelial cells. *Nat. Toxins* 3, 119–128.

Khan, S.A., Wickstrom, M.L., Haschek-Hock, W.M., Schaeffer, D.J., Ghosh, S., Beasley, B.R., 1996. Microcystin-LR-induced alterations in the cytoskeleton of cultured hepatocytes, kidney cells, and fibroblasts. *Nat. Toxins* 4, 217–220.

Kerr, J.F.R., Wyllie, A.H., Currie, A.R., 1972. Apoptosis: a basic biological phenomenon with wide-ranging implications in tissue kinetics. *Br. J. Cancer.* 26, 239–257.

Kotak, B.G., Zurawell, R.W., Prepas, E.E., Holmes, C.F.B., 1996. Microcystin-LR concentration in aquatic food web compartments from lakes of varying trophic status. *Can. J. Fish. Aquat. Sci.* 53, 1974–1985.

Liang, Y.L., 1981. The apparatus of filtering and feeding of silver carp and bighead carp. *J. Dalian. Fish. Coll.* 1, 13–33 (in Chinese).

- Li, X.Y., Liu, Y.D., Song, L.R., 2001. Cytological alterations in isolated hepatocytes from common carp (*Cyprinus carpio* L.) exposed to microcystin-LR. *Environ. Toxicol.* 16, 517–522.
- Li, X.Y., Chung, I.K., Kim, J.I., Lee, J.A., 2004. Subchronic oral toxicity of microcystin in common carp (*Cyprinus carpio* L.) exposed to microcystin under laboratory conditions. *Toxicon* 44, 821–827.
- Malbrouck, C., Trausch, G., Devos, P., Kestemont, P., 2003. Hepatic accumulation and effects of microcystin-LR on juvenile goldfish *Carassius auratus* L. *Comp. Biochem. Physiol. C* 135, 39–48.
- McDermott, C.M., Nho, C.W., Howard, W., Holton, B., 1998. The cyanobacterial toxin, microcystin-LR can induce apoptosis in a variety of cell types. *Toxicon* 36, 1981–1996.
- Miura, G.A., Robinson, N.A., Geisbert, K.A., Bostian, J.D.W., Pace, J.G., 1989. Comparison of in vivo and in vitro toxic effects of microcystin-LR in fasted rats. *Toxin* 27, 1229–1240.
- Opuszynski, K., Shireman, J.V., 1995. *Merbivorous Fishes-Culture and use for weed management*. CRC press, Florida, USA.
- Råbergh, C.M.I., Bylund, G., Eriksson, J.E., 1991. Histopathological effects of microcystin-LR, a cyclic peptide toxin from the cyanobacterium (blue-green alga) *microcystis aeruginosa*, on common carp (*Cyprinus carpio* L.). *Aquat. Toxicol.* 20, 131–146.
- Runnegar, M.T., Kong, S., Berndt, N., 1993. Protein phosphatase inhibition and in vivo hepatotoxicity of microcystins. *Am. J. Physiol.* 265, 224–230.
- Sahin, A., Tencalla, F.G., Dietrich, D.R., Naegeli, H., 1996. Biliary excretion of biochemically active cyanobacteria (blue-green algae) hepatotoxins in fish. *Toxicology* 106, 123–130.
- Slauson, D.O., Cooper, B.J., 1982. *Mechanism of Disease: A textbook of comparative general pathology*. Williams and Wilkins, Baltimore, MD.
- Tang, Y., 1981. Evaluation of balance between fishes and available fish foods in multispecies fish culture ponds in Taiwan. *Trans. Am. Fish. Soc.* 99, 708–717.
- Tencalla, F., Dietrich, D., 1997. Biochemical characterization of microcystin toxicity in rainbow trout (*Oncorhynchus Mykiss*). *Toxicon* 35, 583–595.
- Wickstrom, M.L., Khan, S.A., Haschek, W.M., Wyman, J.F., Eriksson, J.E., Schaeffer, D.J., Beasley, V.R., 1995. Alterations in microtubules, intermediate filaments, and microfilaments induced by microcystin-LR in cultured cells. *Toxicol. Pathol.* 23, 325–337.
- Wickstrom, M.L., Haschek, W.M., Henningsen, G., Miller, L.A., Wyman, J.F., Beasley, V.R., 1996. Sequential ultrastructural and biochemical changes induced by microcystin-LR in isolated perfused rat livers. *Nat. Toxins* 4, 195–205.
- Wyllie, A.H., Kerr, J.F.R., Currie, A.R., 1980. Cell death: the significance of apoptosis. *Int. Rev. Cytol.* 68, 251–305.
- Xie, L.Q., Xie, P., Ozawa, K., Honma, T., Yokoyama, A., Park, H.D., 2004. Dynamics of microcystins-LR and -RR in the phytoplanktivorous silver carp in a sub-chronic toxicity experiment. *Environ. Pollu.* 127, 431–439.
- Xie, P., Liu, J.K., 2001. Practical success of biomanipulation using filter-feeding fish to control cyanobacteria blooms: synthesis of decades of research and application in a subtropical hypereutrophic lake. *Sci. World J.* 1, 337–356.
- Zimba, P.V., Khoo, L., Gaunt, P.S., Brittain, S., Carmichael, W.W., 2001. Confirmation of catfish, *Ictalurus punctatus* (Rafinesque), mortality from Microcystis toxins. *J. Fish. Dis.* 24, 41–47.